BIOCHEMICAL PHARMACOLOGY 73 (2007) 405–416

available at www.sciencedirect.com

ScienceDirect

journal homepage: www.elsevier.com/locate/biochempharm

Irreversible inhibition of glucose-6-phosphate dehydrogenase by the coenzyme A conjugate of ketoprofen: A key to oxidative stress induced by non-steroidal anti-inflammatory drugs?

Carine Asensio [a], *Nicolas Levoin* [a,1], *Cécile Guillaume* [a], *Marie-Justine Guerquin* [a], *Koukeb Rouguieg* [a], *Françoise Chrétien* [b], *Yves Chapleur* [b], *Patrick Netter* [a], *Alain Minn* [a], *Françoise Lapicque* [a,*]

[a] *UMR 7561 CNRS-UHP, Physiopathologie et Pharmacologie Articulaires, Faculté de Médecine, BP 184, F-54505 Vandoeuvre les Nancy, France*

[b] *UMR 7565, Nancy-Université, CNRS, Groupe SUCRES, BP 239, F-54506 Vandoeuvre les Nancy, France*

ARTICLE INFO

Article history:
Received 20 July 2006
Accepted 26 September 2006

Keywords:
Glucose-6-phosphate dehydrogenase
Chiral NSAID
Coenzyme A metabolite
Oxidative stress
Digestive side-effects
Allosteric site

ABSTRACT

Oxidative damage by non-steroidal anti-inflammatory drugs (NSAIDs) has been considered relevant to the occurrence of gastro-intestinal side-effects. In the case of chiral arylpropionate derivatives like ketoprofen (KPF), this mechanism has been evidenced for the R-enantiomer, especially when chiral inversion was observed, and lets us suppose the involvement of CoA conjugates. Glucose-6-phosphate dehydrogenase (G6PD) is the crucial enzyme to regenerate the GSH pool and maintain the intracellular redox potential. This enzyme is known to be down-regulated by palmitoyl-CoA thioester. We hypothesised then that G6PD is the target of carboxylic NSAIDs, *via* their CoA metabolites. We used molecular docking to localise a putative site in the human G6PD then we chose the Yeast orthologue, as the most suitable species to study experimentally the precise molecular interaction. KPF–CoA was effectively shown to bind covalently to the unique cysteine residue of the yeast enzyme. Binding was found to occur in the same site as palmitoyl-CoA. It was decreased in the presence of an allosteric inhibitor of G6PD, phospho(enol)pyruvate, and was not detected with G6PD of *Leuconostoc mesenteroides*, which does not possess the allosteric site. This site is distinct from the catalytic site, and probably allosteric, explaining the observed non-competitive inhibition of its activity by KPF–CoA. KPF–CoA was shown to induce the production of reactive oxygen species in Caco-2 cells, where its inhibition of G6PD activity was observed.

* *Corresponding author*. Tel.: +33 383 68 39 54; fax: +33 383 68 39 59.
E-mail address: Francoise.Lapicque@medecine.uhp-nancy.fr (F. Lapicque).
[1] Present address: Bioprojet-Biotech, F-35762 Saint-Grégoire, France.

Abbreviations: COX, cyclooxygenase; DHEA, dehydroepiandrosterone; G6PD, glucose-6-phosphate dehydrogenase; KPF, ketoprofen; NAK, non-acylating analogue of KPF–CoA; NSAID, non-steroidal anti-inflammatory drugs; PEP, phospho(enol)pyruvate monopotassium; ROS, reactive oxygen species

0006-2952/$ – see front matter
doi:10.1016/j.bcp.2006.09.026

1. Introduction

Non-steroidal anti-inflammatory drugs (NSAIDs) are widely used for their antiphlogistic and analgesic properties. Despite a variable chemical structure, they share the same mechanism of action, relying upon the inhibition of the cyclooxygenases (COXs) involved in the synthesis of prostaglandins. The two isoforms of the enzyme are implied in various physiological processes, such as gastro-intestinal homeostasis (mainly COX-1), and in pathological conditions, such as inflammation (mainly COX-2). The inhibition of the inducible enzyme COX-2 has then been thought to be responsible for the beneficial properties of NSAIDs, while blocking the housekeeping functions of COX-1 would contribute to their gastro-intestinal side effects. Nevertheless, these roles attributed to both COXs appear today to be not so clearly delineated, since COX-1 is also involved in inflammation [1], whereas COX-2 is also involved in intestinal homeostasis [2].

Ketoprofen (KPF), like the other arylpropionic derivatives, is a chiral compound due to the presence of an asymmetric carbon, and marketed as the racemic mixture of *R*- and *S*-enantiomers. The *R*-isomer is known to convert to its antipode *in vivo*, extensively in several animal species [3], and at a rate of 10% in human [4]. The anti-inflammatory effect results almost exclusively from the *S*-enantiomer, the better inhibitor of COXs [5], whereas its antipode possesses in human analgesic properties independent of COX inhibition [6]. In rats, where chiral inversion is important, racemate and *R*-KPF exhibit a higher intestinal toxicity than the *S*-isomer, correlated with a higher oxidative damage and a decreased glutathione level [7]. Generation of reactive oxygen species (ROS) and associated apoptosis were shown to induce gastrointestinal toxicity, apparently unrelated to inflammation [8], and to reduce colon cancers [9]. Therefore, oxidative stress in the gastro-intestinal tract is increasingly considered to lead both to ulcers and to regression of cancer.

Taken together these observations suggest the implication of pathways other than COX inhibition, and/or the participation of the metabolites issued from chiral inversion. In fact, the inhibition of COX by the coenzyme A conjugate of KPF was observed in macrophages and endothelial cells [10]. Searching for pharmacological targets of NSAIDs involved in the regulation of oxidative stress, we focused on proteins known to be regulated by endogenous acyl-CoA derivatives, and among them, on glucose-6-phosphate dehydrogenase, G6PD.

This housekeeping cytosolic protein is the first and rate-limiting enzyme of the pentose phosphate pathway, which uses 6-carbon sugars to give 5-carbon sugars, like ribose for the synthesis of nucleotides and nucleic acids. More precisely, G6PD catalyses the transformation of α,D-glucose-6-phosphate issued from glycolysis, to 6-phosphoglucono-γ-lactone. In the same time, the cofactor $NADP^+$ is reduced to NADPH, which is required for fatty acid synthesis and protection against oxidative stress. G6PD is down-regulated by NADPH itself, and by palmitoyl-CoA [11].

Therefore, the aim of this study was to assess the interaction of the CoA conjugate of KPF (KPF–CoA) with G6PD. A non-acylating analogue of KPF–CoA, NAK (Fig. 1), was also evaluated, in order to assess the contribution of the reactive thioester function. The interaction was characterised on purified enzyme and its consequence on the oxidative state was further studied in Caco-2 cells.

2. Experimental procedures

2.1. Materials

G6PD (EC 1.1.1.49) from *Saccharomyces cerevisiae* (Baker's yeast) (grade II), and from *Leuconostoc mesenteroides*, $NADP^+$, and glucose-6-phosphate were purchased from Roche-Boehringer (Meylan, France). Tris–HCl buffer, glycine, Triton X-100, CoA, KPF, hydroxylamine, *N*-ethylmaleimide, ammonium persulfate, phospho(enol)pyruvate monopotassium (PEP), palmitoyl-CoA, menadione (2-methyl-1,4-naphthoquinone), 6-phospho-

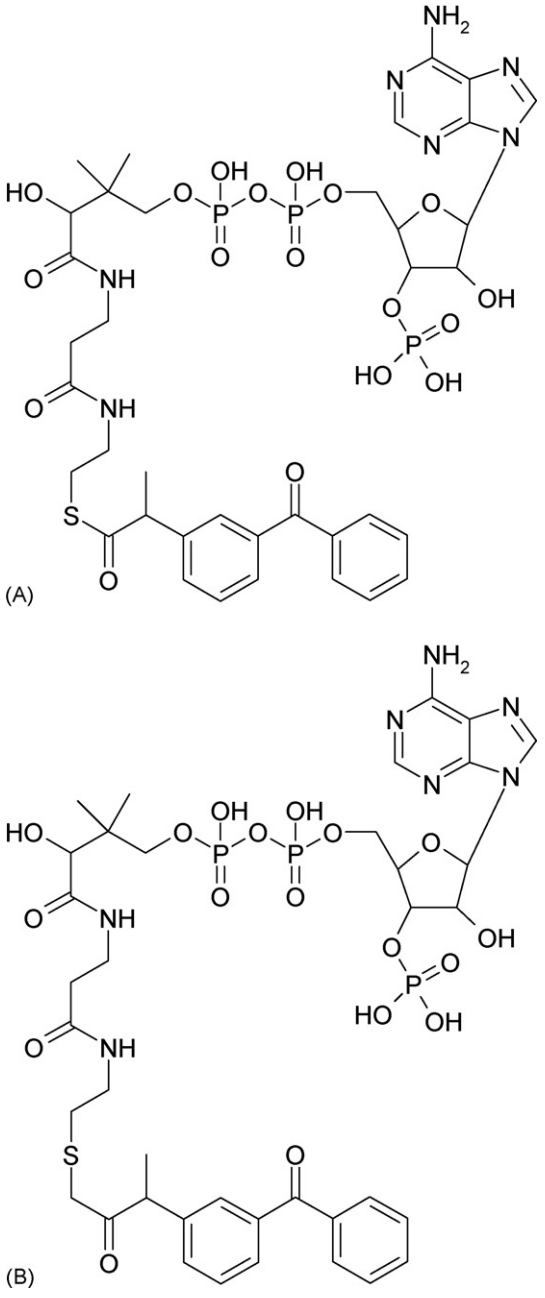

Fig. 1 – Chemical structures of KPF–CoA (A) and NAK (B).

gluconate, dihydrorhodamine-123 (DHR-123), bovine serum albumin (BSA), nitroblue tetrazolium salt/5-bromo-4-chloro-3-indolyl phosphate (NBT/BCIP) and Tween-20® were obtained from Sigma–Aldrich (St. Quentin Fallavier, France). Dimethylsulfoxide (DMSO), magnesium sulfate and bromophenol blue were from Merck (Fontenay sous Bois, France). EDTA, acrylamide/bis-acrylamide and the cell culture media were from Gibco (Cergy Pontoise, France), sodium dodecylsulfate (SDS) and Temed® from Interchim (Montluçon, France). Glycerol was provided by Prolabo (Paris, France), and phosphate buffer saline (PBS) by Eurobio (Les Ulis, France).

(*R*,*S*)-KPF–CoA, and its non-acylating analogue, NAK, were synthesised chemically, as previously described [12].

Anti-KPF polyclonal antibody was obtained from rabbits immunized against KPF-thyreoglobuline by the method described by Maire-Gauthier et al. [13]. Secondary goat anti-rabbit IgG conjugated to alkaline phosphatase were purchased from Sigma.

2.2. Effect of KPF–CoA on purified protein

2.2.1. Enzyme activity

Enzyme activity was assessed by following the reduction of $NADP^+$ to NADPH at 340 nm on a UV-1601 Shimadzu spectrophotometer (Roucaire, Courtaboeuf, France), according to the method previously described by Noltmann et al. [14].

The activity of G6PD was measured for various concentrations of glucose-6-phosphate in the range 1.98×10^{-5} to 1.60×10^{-3} M. In a cuvette containing 500 μL 0.1 M Tris–HCl buffer pH 8.0, 0.15 M magnesium sulfate, and 3.3×10^{-4} M $NADP^+$, thermostated at 37 °C, were added 0.01 μg enzyme in 10 μL, and glucose-6-phosphate. In competition experiments, the enzyme was previously incubated for 1 or 10 min with one of the following compounds: KPF, CoA and KPF–CoA each at 2×10^{-4} or 4×10^{-4} M, NAK at 10^{-3} M, albumin at 1 g/L, SDS at 1% (w/v), hydroxylamine at 1.2 mM.

2.2.2. Adduct formation

The incubation of 5 μg G6PD with KPF–CoA at a concentration variable between 0.1 and 1 mM, was studied in 50 mM phosphate buffer pH 7.4. For competition studies, several compounds were incubated with 5 μg enzyme before further incubation with KPF–CoA: glucose-6-phosphate, $NADP^+$, NAK, each at 5×10^{-4} M; palmitoyl-CoA from 0.01 to 1 mM and PEP at 1 and 2 mM. In other experiments, 1% SDS or *N*-ethylmaleimide at a concentration varying from 2×10^{-4} to 2×10^{-3} M, were added before the incubation of the enzyme with 5×10^{-4} M KPF–CoA. Conversely, 0.726 M hydroxylamine was added after incubation.

SDS-PAGE was performed using 9 and 5% (w/v) acrylamide for separating and stacking gel, respectively. Proteins were transferred onto Immobilon P membrane (Millipore, Bedford, MA) by liquid electroblotting, using a glycine/Tris/0.1% (v/v) methanol buffer adjusted to pH 7.4 for 50 min at 80 V. Blots were saturated with 3% (w/v) BSA in 0.02% (w/v) Tween-20® in PBS. Immunodetection was performed using anti-KPF polyclonal antibody diluted 1:5000 v/v and the secondary goat anti-rabbit IgG alkaline phosphatase conjugated 1:5000 v/v. Densitometry was performed on a Gel Doc 2000 apparatus (Bio Rad, Marnes la Coquette, France). A systematic control was done by colouring the membranes with Coomassie blue solution to assert that the same quantity of protein was deposed in each well and that the revelation was specific to bound KPF.

2.2.3. Data analysis

The activity of the enzyme was analysed using the Michaelis–Menten's equation, as proposed previously [15]:

$$V = \frac{V_{max} \times [S]}{K_m + [S]}$$

where V is the initial rate of the reaction measured for the substrate concentration [S]; K_m and V_{max} are the kinetic parameters of the enzyme. k_{cat} was deduced from V_{max} and enzyme concentration.

The presence of a competitor at the concentration [*I*] led to an inhibition of the activity, and was quantified by the inhibition constant, K_i. The mechanism of this inhibition can be either competitive, non-competitive, or uncompetitive; the respective variations of initial rate with [S] are then expressed by the following equations:

$$V = \frac{V_{max}[S]}{K_m(1 + [I]/K_i) + [S]} \qquad V = \frac{(V_{max}/1 + [I]/K_i)[S]}{K_m + [S]}$$

$$V = \frac{V_{max}[S]}{K_m + (1 + [I]/K_i)[S]}$$

Fitting of the experimental data to one model was carried out by minimisation of the objective function, defined as the sum of square deviations between calculated and experimental data. The best fit was with a weight at 1/*Y*. These equations were used to fit the rate–concentration curves and to estimate the values of the parameters, K_m and k_{cat}.

2.3. Effect of KPF–CoA on Caco-2 cells

2.3.1. Culture of Caco-2 cell line

Human colon carcinoma cells, Caco-2 (ECACC, Salisbury, UK), were grown in Dulbecco's modified Eagle's medium containing 2 mM L-glutamine, 1 mM sodium pyruvate, 100 μg/mL streptomycin, 100 U/mL penicillin and 10% fetal bovine serum (FBS) in a humidified atmosphere of 5% CO_2 at 37 °C.

2.3.2. Measurement of the intracellular ROS production

All treatments were applied to confluent culture in triplicate. Culture medium was removed and cells were rinsed with PBS. FBS-free medium was added for 6 h. Cells were exposed to various concentrations of KPF–CoA (10^{-5}, 5×10^{-5} and 10^{-4} M) diluted in PBS for 30 min. Positive control was obtained with 15 μM menadione diluted in PBS containing 0.1% (v/v) DMSO for 15 min. Control cells were incubated with PBS alone and PBS containing the vehicule (0.1% (v/v) DMSO).

ROS production was measured using the oxidant-sensitive DHR-123 dye, as previously described [16]. This compound is able to easily cross cell membranes and, upon oxidation by ROS, turns into fluorescent rhodamine-123. Caco-2 cells were plated on 6-wells plates. Cell cultures were treated with KPF–CoA or menadione and were further incubated with 5 μM DHR-123 for 5 min before the end of the treatment. The cells were rinsed with PBS before being scraped off with a lysis buffer containing

10 mM Tris–HCl pH 7.4 and 0.5% Tween-20®, v/v. The homogenate was centrifuged at 10,000 × *g* for 10 min. The supernatant was then subjected to a spectrophotometric analysis to measure the rhodamine-123 fluorescence with excitation and emission wavelengths, 500 and 531 nm, respectively.

2.3.3. *Measurement of intracellular G6PD activity*

Similar experiments were performed to determine G6PD activity. Cells were exposed to various concentrations of KPF–CoA (10^{-6}, 5×10^{-6}, 10^{-5}, 5×10^{-5} and 10^{-4} M) or palmitoyl-CoA (10^{-6}, 10^{-5}, 5×10^{-5} and 10^{-4} M) diluted in PBS for 30 min. Controls were obtained with 10^{-4} M KPF diluted in PBS containing 0.1% (v/v) DMSO and 10^{-4} M CoA diluted in PBS for 30 min. Negative control cells were incubated with PBS alone and PBS containing the vehicule (0.1% (v/v) DMSO). Activity was measured by following the generation of NADPH at 340 nm on a spectrophotometer, according to the method described by Stanton et al. [17].

As 6-phosphogluconate dehydrogenase (6PGD) is also involved in the generation of NADPH, both 6PGD and total dehydrogenase activity (G6PD + 6PGD) were determined independently. G6PD activity was then obtained by deducting 6PGD activity from total dehydrogenase activity. The reaction mixture (500 μL) contained (all at final concentration) 50 mM Tris–HCl buffer, pH 8.1, 1 mM $MgCl_2$, 800 μM glucose-6-phosphate and/or 800 μM 6-phosphogluconate and 100 μL protein extract. The enzyme reaction was triggered by the addition of 400 μM $NADP^+$ and monitored for up 3 min at 340 nm.

The measured rate was converted into international units (IU—μmol NADPH/(min mg protein)), and expressed as a percent of control.

2.4. *Molecular modelling*

The X-ray structure of Human G6PD (PDB:1QKI, 2BHL and 2BH9) [18,19] were used and compared with *L. mesenteroides* (PDB:1DPG, 1E7Y) [20,21].

The entire monomer of human G6PD was investigated in search of a possible KPF binding site. Using LigandFit (Cerius2 v 4.1, Accelrys, San Diego, CA) as a probe, the five largest sites were selected and tested for KPF docking ability. In each site, five partitions were allowed to dock a collection of pre-computed conformers of the compound. Poses were minimized with CFF force field and a non-bond energy cut off of 16 Å, with a distance dependent dielectric of 1, and their docking score evaluated using LIGSCORE-2 scoring function (Table 1).

The first site corresponds to the active site and was not considered because of overlap with substrate binding sites.

Table 1 – Molecular docking of KPF in human G6PD

Site number	Accessible volume (Å^3)	⟨LIG-2⟩ top 10 poses
1	3079	5.4
2	898	3
3	614	4.9
4	563	5.1
5	287	≪0
6	333	≪0

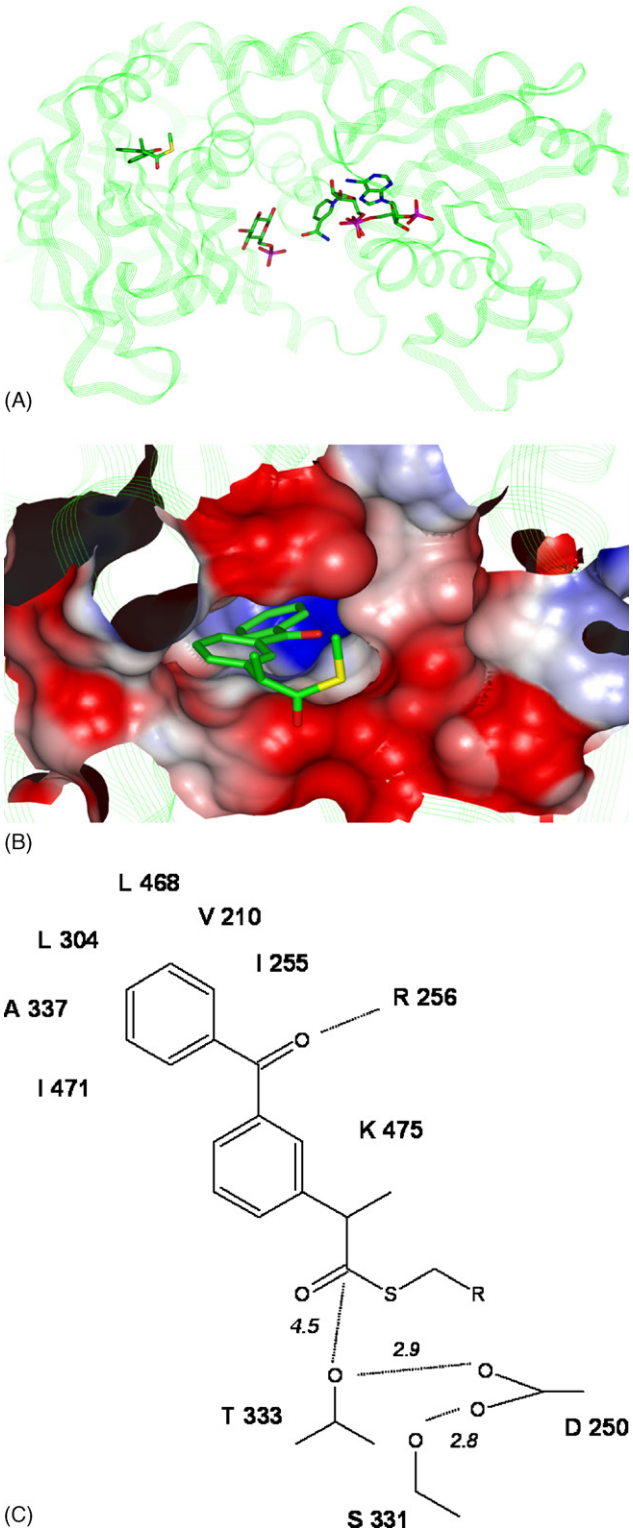

Fig. 2 – Energy-minimized structure of the complex between G6PD and KPF–CoA (PDB#1QKI, 2BHL, and 2BH9) [18,19]. (A) Location of the KPF–CoA in human G6PD in view of the active site: G6P and NADP, respectively, shown from PDB:2BHL and PDB:2BH9; (B) detail of the proposed KPF–CoA binding site in human G6PD. The Connolly surface is coloured according to the electrostatic potential as determined using DELPHI; (C) schematic drawing of the KPF–CoA binding site with important residues labelled.

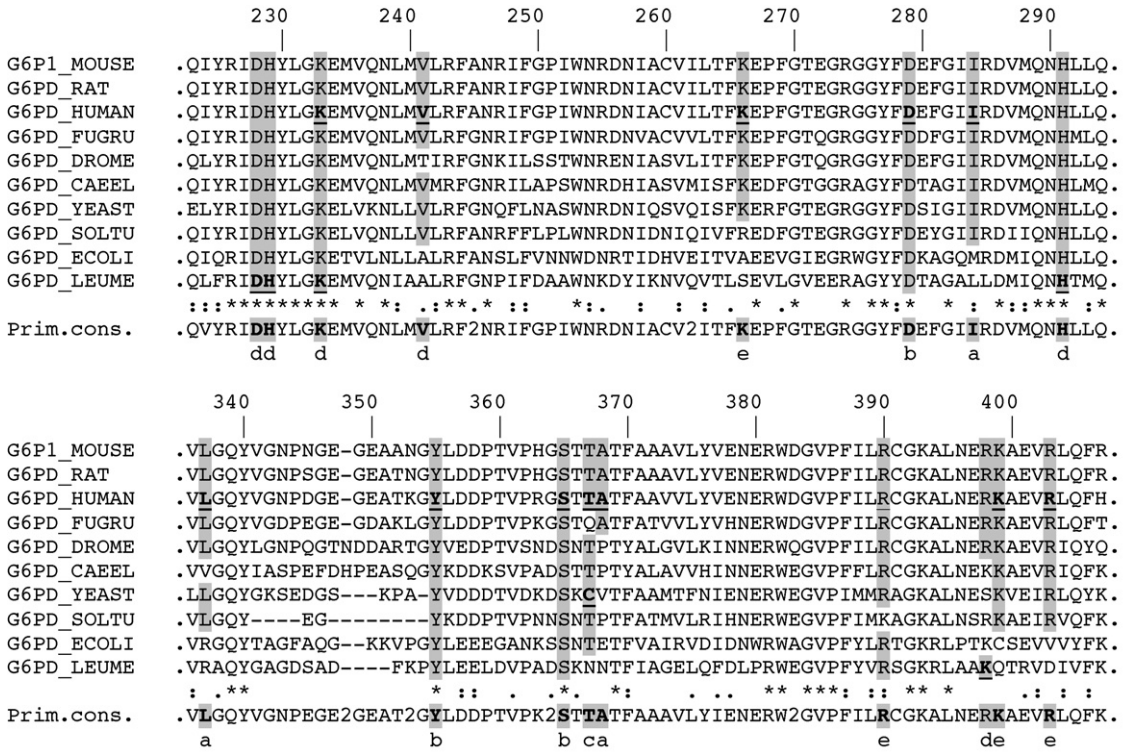

Fig. 3 – Alignment of sequences of G6PD from several species (Swiss Protein Database): MOUSE, *Mus musculus* (Q00612); RAT, *Rattus norvegicus* (P0537); HUMAN, Homo sapiens (P11413); FUGRU, *Fugu rubripes* (Japanese pufferfish) (P54996); DROME, *Drosophila melanogaster* (fruit fly) (P12646); CAEEL, *Caenorhabditis elegans* (Q27464); YEAST, *Saccharomyces cerevisiae* (Baker's yeast) (P11412); SOLTU, *Solanum tuberosum* (potato) (P37830); ECOLI, *Escherichia coli* (P22992); LEUME, *L. mesenteroides* (P11411). Partial sequences showing the residues interacting with KPF–CoA (a), with thioester function (b and c), and especially the cysteine residue in Yeast G6PD (c), and also the residues involved in the catalytic site and in the structural NADP site, as known for HUMAN [18,19] (d) and LEUME [20,21] (e). (*) identity; (:) strong similarity; (·) weak similarity.

Based on their docking score, site 2 was abandoned and sites 3 and 4 were studied further. The two best poses on each site were kept as alternative binding mode, and minimised following two steps. They were first treated *in vacuo* using a distance dependent dielectric constant of 4, with a cell multipole summation method and 6000 maximum iterations of standard minimization protocol (steepest descent and conjugate gradient) and keeping backbone frozen. Then complexes were solvated by a layer of 15 Å water and minimised using a constant dielectric constant of 1, keeping only the backbone frozen. CFF force field was used for the complete procedure within Discover3.0 (Accelrys). Last, the interaction energy, as described by a van der Walls and a Coulomb term, was calculated. The site that allowed the minimal binding energy was site 3, and the binding mode is illustrated in Fig. 2.

The multiple sequence alignment was performed with CLUSTAL W 1.8 with the GONNET matrix (http://www.pbil.ibcp.fr).

2.5. Statistical analysis

Data were presented as mean ± S.E.M. StatView 5 was used for statistical analysis. To compare the effect of KPF–CoA treatment on ROS production or G6PD activity, raw data were submitted to univariate ANOVA, and PLSD Fisher analysis, and $p < 0.05$ was considered significant.

The distances between amino acids likely to be implicated in the acylation mechanism are specified in Å.

3. Results

3.1. Prediction of interactions

The docking of KPF–CoA was performed in order to evaluate its possible interaction with Human G6PD (PDB#1QKI) [18]. The optimal site is mostly hydrophobic in nature. It lets appear that one phenyl ring of KPF–CoA would be sandwiched in an hydrophobic cavity formed by Ile254 and 255, Ala337, Leu304, Leu468 and Ile471, the benzophenone carbonyl making an hydrogen bond to Arg256, and the other phenyl ring being in contact with the alkyl chain of Lys475 and Thr333 (Fig. 2). In these conditions, the thioester function is in close proximity of hydroxyl of Ser331, Thr333 and Asp250; Thr333 appears as the nearest position from the carbon.

The alignment of the currently known G6PD amino-acids sequences showed a high identity between the human enzyme and many other species of animals, plants and micro-organisms, especially in the catalytic domain (Fig. 3). Interestingly, Yeast G6PD (*S. cerevisiae*) presents a unique cysteine residue in its sequence at the location of Thr333 and *L.*

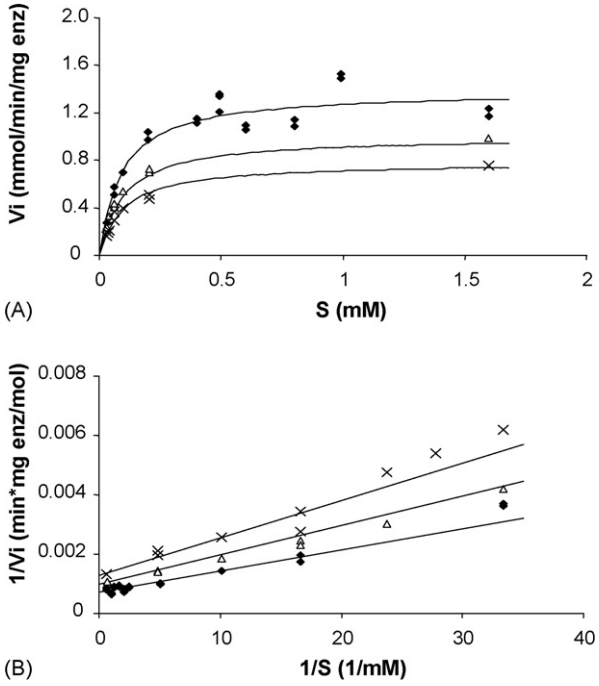

Fig. 4 – Inhibition of G6PD activity by KPF–CoA. (A) Initial rate of reaction (Vi) is reported *vs.* glucose-6-phosphate concentration, after 1 min incubation with buffer (◆) KPF–CoA 2×10^{-4} M (△), KPF–CoA 4×10^{-4} M (×); (B) Lineweaver-Burk representation.

mesenteroides G6PD an asparagine residue at the same location. The sulfhydryl group of cysteine has been frequently shown to be responsible for the conjugation of proteins by CoA thioesters, precisely like for Yeast G6PD by palmitoyl-CoA [22]. Thus we used the Yeast enzyme and *L. mesenteroides* G6PD as a natural form of cysteine-scanning mutagenesis.

3.2. *Characterisation of KPF–CoA interaction with G6PD enzyme*

3.2.1. *Inhibition of enzymatic activity*

The activity of Yeast G6PD for glucose-6-phosphate followed a Michaelis–Menten kinetics (Fig. 4). Fitting of the experimental data gave values for K_m of 0.099 mM and for k_{cat} of 36,000 min^{-1}. These values are in good agreement with those previously published for *L. mesenteroides*, with K_m of 0.114 mM, and k_{cat} of 31,300 min^{-1} [23], and for human placenta, with K_m of 0.04 mM, and k_{cat} of 17,800 min^{-1} [15].

The activity of G6PD was not modified upon addition of either KPF or CoA at 4×10^{-4} M (data not shown), but was strongly inhibited by the conjugate KPF–CoA, by about 50 and 75% for a concentration of KPF–CoA at 2×10^{-4} and 4×10^{-4} M, respectively (Fig. 4). Experimental data obtained for various concentrations of substrate were fitted by the usual models of competitive, non-competitive and uncompetitive inhibition. The best fit was obtained for a non-competitive inhibition, with K_i equal to 0.52 mM (Fig. 4).

The inhibition was not significantly modified after incubating KPF–CoA for 1 and 10 min (Table 2). It was not reversed by the addition of 1 g/L albumin, a protein known to exhibit a very high affinity for the conjugate [24], and one would therefore expect to observe a recovery in activity of G6PD if the inhibition is reversible. By contrast, the inhibition was partially reversed after addition of hydroxylamine. Taken together, these results showed a rapid irreversible inhibition of G6PD by KPF–CoA, and suggested the implication of a cysteine residue.

The activity of G6PD was inhibited by NAK, but to a lower extent than by KPF–CoA, since the initial velocity was reduced only by 27% for a concentration of NAK at 10^{-3} M (Table 2). About half of inhibition was recovered upon addition of albumin, in accordance with a reversible inhibition process.

3.2.2. *Formation of adducts*

The incubation of Yeast G6PD with KPF–CoA led to the formation of adducts, as revealed by immunodetection of bound KPF after Western blot analysis (Fig. 5). Adducts were observed for the lowest concentration used, 10^{-4} M. The extent of this formation increased with the concentration of KPF–CoA, to a plateau observed from 4×10^{-4} M (Fig. 5A). The formation was rapid and stable, since adducts were observed even at the first experimental time of 1 min, and were present to a constant extent for at least 2 h after incubation (Fig. 5B). A similar reactivity was observed for KPF–CoA with COXs and led also to the enzyme inactivation within 2 min [10].

The native structure of the protein is required since the formation of adducts was not observed after G6PD thermal denaturation at 100 °C for 10 min (data not snown). Conversely, the extent of adduct formation was increased in the presence of SDS (Fig. 5C), which is known to inhibit G6PD activity, by converting the native tetramer into inactive monomers [11]. This suggests that this dissociation renders this domain more accessible to the conjugate. Alternatively,

Table 2 – Inhibition of G6PD activity by KPF–CoA and NAK

	Incubation time (min)		Albumin	Hydroxylamine
	1	10		
Control	100	100	99 ± 2	99 ± 2
KPF–CoA 2×10^{-4} M	77 ± 2	77 ± 2	74 ± 3	88 ± 2
KPF–CoA 4×10^{-4} M	68 ± 3	55 ± 3	n.d.	n.d.
NAK 10^{-3} M	73 ± 5	n.d.	88 ± 2	n.d.

Effect of incubation time, and of further addition of 1 g/L albumin or 1.2 mM hydroxylamine. Mean values of initial rates are given as percent of control, with standard deviation for three independent experimentations; n.d.: not determined.

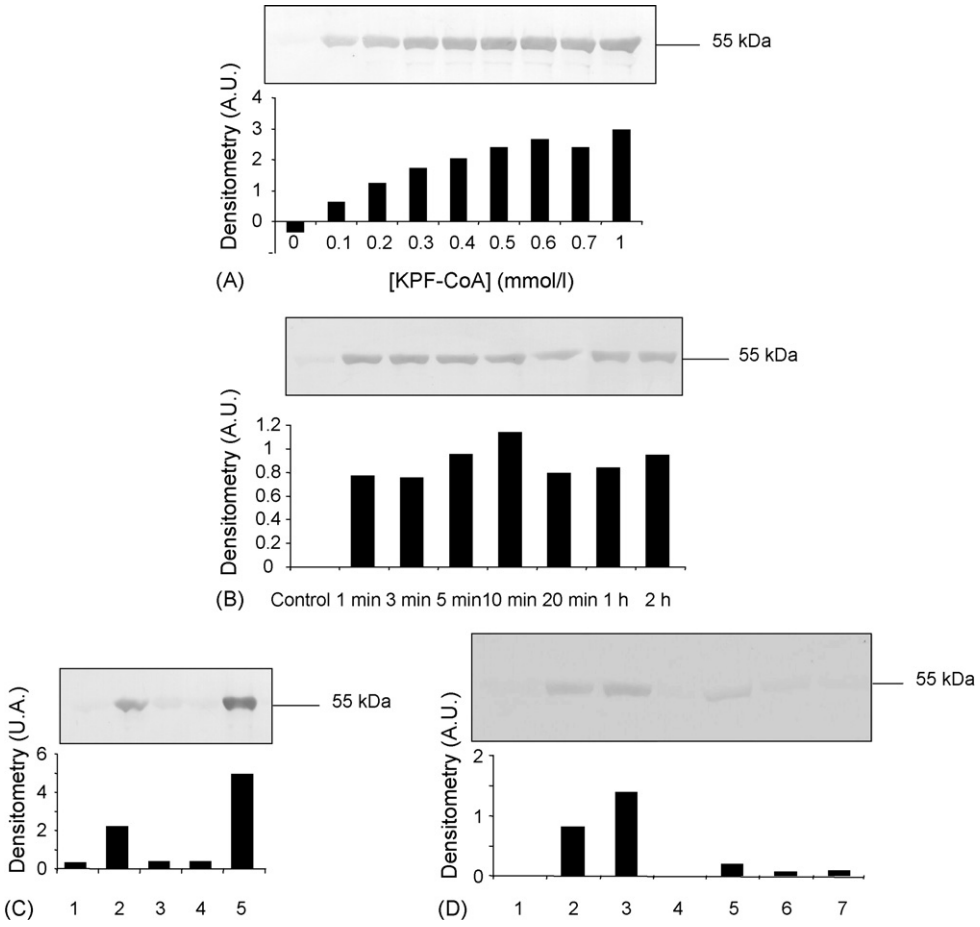

Fig. 5 – Formation of KPF-adducts on G6PD with KPF–CoA at various concentrations after 2 h incubation (A), with KPF–CoA 0.1 mmol/L after various incubation times (B), and effect of hydroxylamine, SDS (C), and *N*-ethylmaleimide (D) on adduct formation of G6PD by KPF–CoA. G6PD (5 μg) were incubated at room temperature. (C) (1): control; 5 μg protein were incubated with KPF–CoA 5×10^{-4} M (2); before addition of hydroxylamine 0.726 M (3); 5 μg protein treated with SDS 1% (4); were incubated with KPF–CoA (5). (D) (1): control, 5 μg protein were incubated with KPF–CoA 2×10^{-4} M (2) and 5×10^{-4} M (3), with *N*-ethylmaleimide 2×10^{-4} M (4), with KPF–CoA 2×10^{-4} M added 20 min after *N*-ethylmaleimide 2×10^{-4} M (5), 6×10^{-4} M (6), 2×10^{-3} M (7). Western blot were revealed by anti-KPF antibody and densitometry is given in arbitrary unit. The panels are representative immunoblots from more than three different analyses.

the deterging properties of SDS may enhance the solubility and then the availability of KPF–CoA for the protein.

The addition of hydroxylamine suppressed the adducts formed after incubation of G6PD and KPF–CoA (Fig. 5C). *N*-Ethylmaleimide, a compound known to protect SH groups, also prevented the enzyme from adduct formation during subsequent incubation with KPF–CoA (Fig. 5D). On the contrary, no adduct was detected after incubation of KPF–CoA with the cysteine-lacking G6PD of *L. mesenteroides* (Fig. 6). This can be rationalised in view of the crystal structures: the equivalent KPF–CoA binding site in G6PD from *L. mesenteroides* is quite different from yeast or human, in term of amino-acid composition. In fact, four hydrophobic residues that appear crucial for KPF binding in our model, are lacking and mutated in polar counterpart: Leu304 (human) is mutated in Arg286 (*L. mesenteroides*), Ala334 in Asn313, Leu468 in Ser447, and Ile471 in Tyr450. As a proof of this shift towards more hydrophilic nature, the crystal structure shows two water molecules in the site of *L. mesenteroides* G6PD (PDB: 1E7Y), but

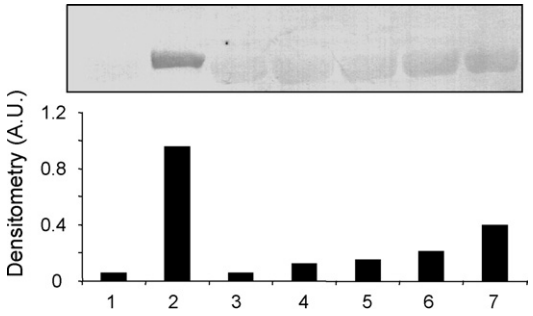

Fig. 6 – Adduct formation with *L. mesenteroides* G6PD. About 5 μg protein were incubated with KPF–CoA and analysed by Western blot with anti-KPF antibody. In comparison to Yeast G6PD without (1) and with 10^{-4} M of KPF–CoA (2), *L. mesenteroides* G6PD without KPF–CoA (3) and with 10^{-4} M (4), 2×10^{-4} M (5), 3×10^{-4} M (6) and 4×10^{-4} M (7) of KPF–CoA.

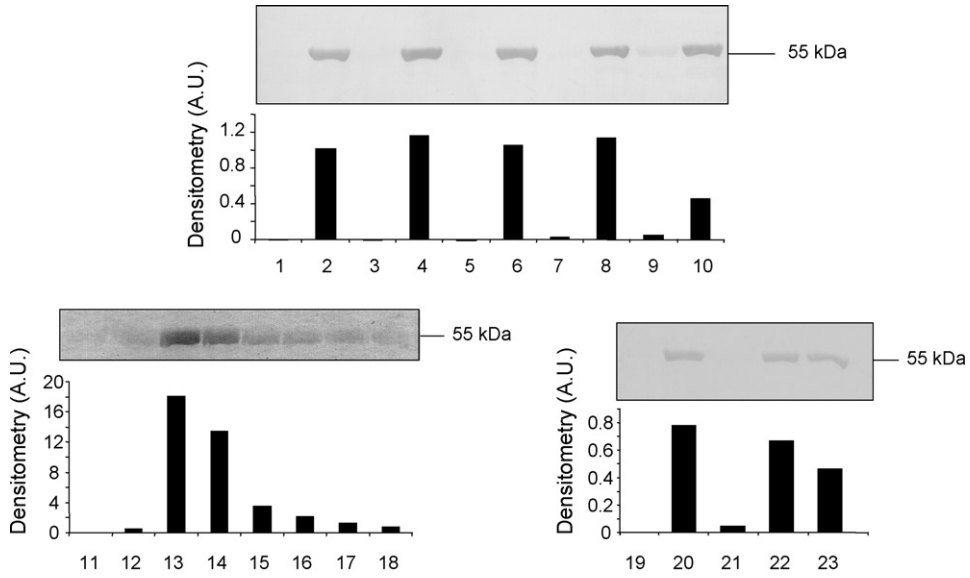

Fig. 7 – Competition of various compounds with KPF–CoA for adduct formation. (1), (11), (19): control; 5 μg protein were incubated with KPF–CoA at 5×10^{-4} M (2), (13), (20), glucose-6-phosphate (3), glucose-6-phosphate and KPF–CoA (4), $NADP^+$ (5), $NADP^+$ and KPF–CoA (6), glucose-6-phosphate and $NADP^+$ (7), glucose-6-phosphate, $NADP^+$ and KPF–CoA (8), NAK (9), NAK and KPF–CoA (10), palmitoyl-CoA 1 mM (12), palmitoyl-CoA 0.01 mM and KPF–CoA (14), palmitoyl-CoA 0.1 mM and KPF–CoA (15), palmitoyl-CoA 0.2 mM and KPF–CoA (16), palmitoyl-CoA 0.5 mM and KPF–CoA (17), palmitoyl-CoA 1 mM and KPF–CoA (18), PEP 1 mM (21), PEP 1 mM and KPF–CoA (22), PEP 2 mM and KPF–CoA (23). Western blot were revealed by anti-KPF antibody and densitometry is given in arbitrary unit. Results of one of two similar experiments are shown.

none in human one. The absence of binding in the case of NAK (Fig. 7), the non-acylating analogue of KPF–CoA in which the thioester group is replaced by a thiomethylene keto group (Fig. 1), further supports the involvement of a thioester bond in the covalent binding of KPF–CoA to G6PD.

NAK inhibited the formation of adducts by about 50% when both compounds were added at the same concentration (Fig. 7), suggesting that KPF–CoA binding occurs in a specific site. Competition experiments were then conducted to characterise this binding site. The co-incubation of the enzyme with its substrate, glucose-6-phosphate, and coenzyme, $NADP^+$, or both together, had no appreciable effect on the formation of adducts (Fig. 7). When G6PD was previously incubated with another compound known to bind a cysteine residue, like palmitoyl-CoA, the concentration of KPF-adducts lowered in a concentration-dependent manner (Fig. 7). Finally PEP, a known allosteric inhibitor of G6PD [25], was found to decrease adduct formation by about 40% at 2 mM of PEP (Fig. 7).

All together, these results suggest that the covalent binding does not occur to the catalytic site, and are in agreement with the non-competitive inhibition observed with respect to glucose-6-phosphate. The adduct formation implies probably the unique cysteine residue of Yeast G6PD, located at the place of Thr333 in the human sequence: this observation confirms the prediction issued from the docking presented above (Fig. 2) and leads us to better characterise this new site in G6PD.

Few binding sites were described for G6PD in the relevant literature. Among them, the active site was particularly investigated for the *L. mesenteroides* G6PD by Vought et al. [26], using site-directed mutagenesis and X-ray analysis, and evidenced the role of particular amino-acids in substrate and coenzyme binding: His240 (position 291 in the alignment of Fig. 3) is the catalytic base, Lys343 (398) and Lys182 (233) are important in substrate binding, whereas Arg46 (89) and Lys343 (398) determine the coenzyme specificity. With the exception of the last residue, the other ones are conserved in the alignment, and some of them were found also concerned by the catalysis in the human enzyme [19]. For this last enzyme, a second molecule of $NADP^+$ is bound to a structural site, allowing the good stability of the enzyme together with Asp421 (459). This site involves the following residues: Lys238 (266), Arg357 (390), Asn363 (396), Glu364 (397), Lys366 (399), Arg370 (403), Tyr401 (437), Asp421 (459), Arg487 (526), Tyr503 (542), and Trp509 (550), in the close vicinity of the catalytic site.

The site of KPF–CoA involves the side-chains of Ile253, Ile254, Arg255, while their backbones are in the catalytic site. So even a small conformational movement induced by a ligand in the site we propose might have an effect in the catalytic efficiency. This site does not exist in *L. mesenteroides*, since neither KPF–CoA in our study (Fig. 6) nor palmitoyl-CoA in a previous study [11] was bound to the protein. The site binds also PEP, an allosteric inhibitor, previously shown able to force the enzyme to display a sigmoid response to glucose-6-phosphate [25]. Interestingly, the allosteric site was shown for G6PD of various species, except that of *L. mesenteroides* [27]. In human, the kinetics is sigmoid for the intracellular enzyme, but obeys a Michaelis–Menten's law for the purified enzyme [28]; the discrepancy was explained as arising from aggregation states of the enzyme higher than dimer and tetramer [15]. In our study, the kinetics was hyperbolic, but

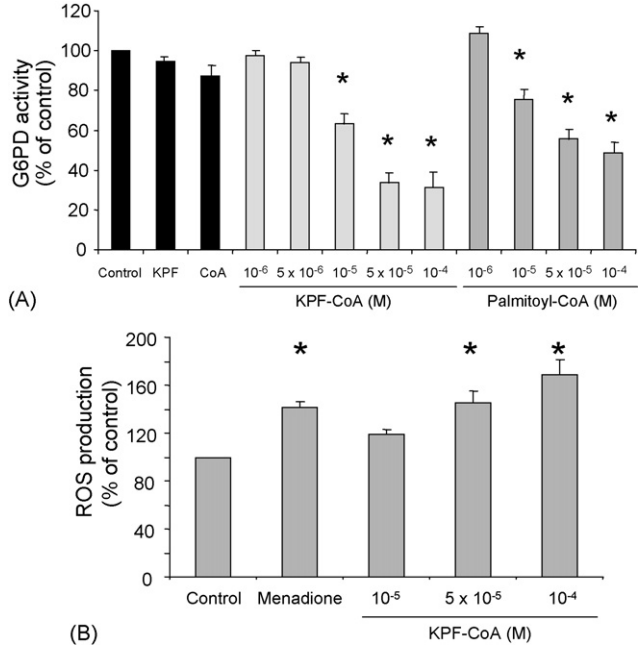

Fig. 8 – Effect of KPF–CoA on Caco-2 cells. (A) Effect of KPF–CoA and palmitoyl-CoA on G6PD activity in Caco-2 cells. Confluent Caco-2 cells were incubated without (control) or with KPF at 1×10^{-4} M, CoA at 1×10^{-4} M, KPF–CoA and palmitoyl-CoA each at different concentrations for 30 min. G6PD activity was measured in the supernatant of lysed cells, as explained in Section 2. (B) Effect of KPF–CoA on ROS production in Caco-2 cells. Confluent Caco-2 cells were incubated without (control) or menadione as a positive control, or with KPF–CoA for 30 min. ROS production was measured in lysed cells by the rhodamine-123 fluorescence. $^{*}p < 0.05$ compared to control value.

low deviations may be difficult to assess [15]. Palmitoyl-CoA was shown to bind the same site as KPF–CoA. Owing to the role of palmitoyl-CoA in the regulation of activity, it may then be speculated that the site of KPF–CoA described in this study, corresponds to the allosteric site.

3.3. *In vitro effect of KPF–CoA on Caco-2 cells*

Confluent Caco-2 cells were incubated with various concentrations of KPF–CoA for 30 min.

The activity of G6PD decreased with increasing concentration of KPF–CoA, and inhibition was significant above 10^{-5} M (Fig. 8A). This inhibition was not observed for KPF or CoA alone, and was found also for palmitoyl-CoA, but to a lower extent than with KPF–CoA (Fig. 8A). The later result is in agreement with the well-known inhibitory effect of palmitoyl-CoA [11,22].

The production of ROS was increased concomitantly to activity inhibition and the difference was found dose-dependent and significant for KPF–CoA concentrations higher than 5×10^{-5} M (Fig. 8B). Similarly G6PD inhibition by diphenyleneiodonium induced ROS production in N11 cells [29]. In cardiomyocytes, G6PD was found essential for maintenance of cytosolic redox status, as determined by the production of ROS associated by depletion of cytosolic GSH level and G6PD inhibition [30].

4. Discussion

Apoptosis induced by NSAIDs was first thought to be due to COX inhibition, especially of COX-2, after the effects of celecoxib, a selective COX-2 inhibitor, were evaluated on colonic carcinogenesis in rats [31]. However, the effects on intestinal polyposis of compounds which do not inhibit COX, such as the *R*-enantiomer of flurbiprofen [32], of sulindac sulfone on colon carcinogenesis [33], and also of *R*-KPF on gastro-intestinal toxicity [7], suggested the existence of additional mechanisms independent of COX, not elucidated until now, and probably related to the formation of ROS [34].

NSAIDs were shown to affect mitochondrial energy metabolism and oxidative phosphorylation, leading to increased ROS production, swelling of mitochondrial membrane, and then to apoptosis. In the case of arylpropionates, the carboxylic function leads to uncoupling oxidative phosphorylation (Fig. 9). Its correlation with pK_a [35] seems then perfectly logical, as well as the similar effect on mitochondrial respiration exhibited by both enantiomers of ibuprofen, which have the same pK_a value [36]. The higher toxic effect of the *R*-enantiomer on the mitochondrial functions was then explained by the stereoselective inhibition of beta-oxidation displayed by *R*-ibuprofen, attributed to the competition for CoA pool. It can also be due to the inhibition of acetyl-CoA carboxylase by CoA conjugate, as observed for ibuprofen [37], and to incorporation into membranes as a hybrid triglyceride [38]. Interestingly, in this last study, lipid peroxidation was correlated with a decreased content in GSH and an increased level of its oxidised form (GSSG). The same result was observed with other arylpropionates, and recently with *R*-KPF, associated with a higher level of ROS [9]. Moreover, diclofenac and mefenamic acid induced a substantial decrease in the mitochondrial NADPH levels [39].

Elimination of ROS is mainly attributed to GSH reacting with hydrogen peroxide (H_2O_2). During this reaction GSH is oxidised to GSSG. Its recycling by glutathione reductase depends on the cofactor, NADPH. In mammals, most of NADPH is produced by the pentose phosphate pathway and more precisely by G6PD [40]. G6PD becomes more important for cell survival during oxidative stress, since in normal situations cells can survive by using reducing equivalents produced by G6PD-independent pathways. The activity of this enzyme plays a critical role for regulation of the intracellular redox level also during cell growth. Its activity is increased by a moderate oxidative stress, but is strongly inhibited in severe oxidative stress, leading to molecular damage mediated by the oxidation of protein thiols [41].

As a crucial enzyme, G6PD is regulated by different ways and molecules. Palmitoyl-CoA and the product NADPH down-regulate its activity [11,15,22], and PEP is an allosteric inhibitor [25]. 4-Hydroxy-2-nonenal, one of the major products of membrane lipid peroxidation, was shown to bind to *L. mesenteroides* G6PD on a lysyl residue and to induce a non-competitive inhibition of its activity [42]. The effects of very few drugs were assessed on G6PD. Cefaperazone/sulbactam

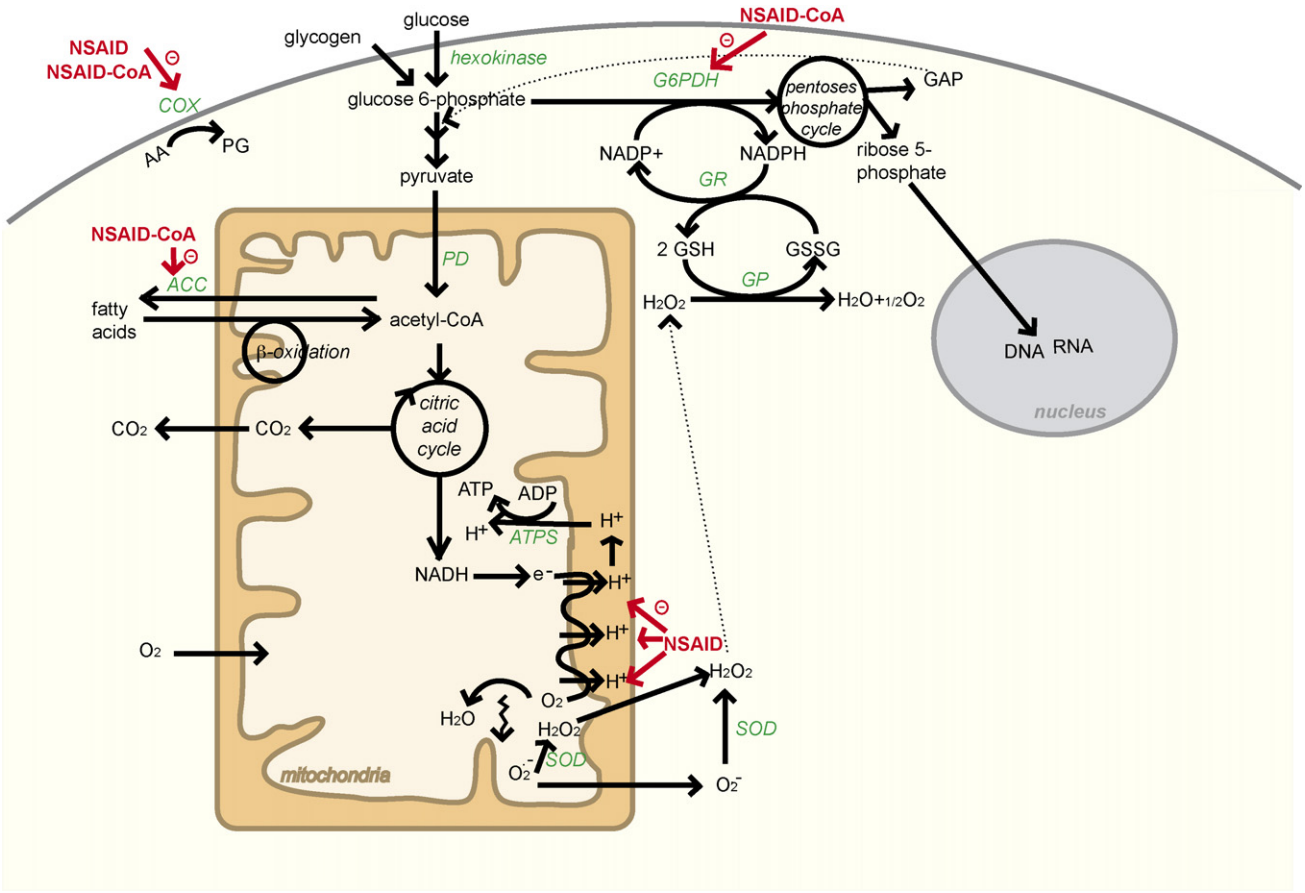

Fig. 9 – Main cellular pathways involved with G6PD and oxidative stress, and interactions with NSAIDs or their CoA conjugates, as observed from this study and [10,35,37]. AA, arachidonate; ACC, acyl-CoA carboxylase; ATPS, ATP-synthase; GAP, glyceraldehyde-3-phosphate; GP, glutathion peroxydase; GR, glutathion reductase; GSH, reduced glutathion; GSSG, oxidised glutathione; PD, pyruvate dehydrogenase; PG, prostaglandin; SOD, superoxyde dismutase.

competitively inhibited the enzyme activity in human erythrocytes, whereas ampicillin/sulbactam and metamizol inhibited non-competitively this activity [43,44]. Aspirin inhibited irreversibly Yeast G6PD by covalent attachment to a lysine residue [45], and by comparing the amino-acid sequence of the tryptic peptide containing the reactive residue with the full sequence, it was deduced that binding occurs on the reactive lysine, at position 190 in Yeast, or 205 in Human G6PD. Dehydroisoandrosterone and other steroids are non-competitive inhibitors of mammalian G6PD activity [46]. In a study of allosteric inhibitors of G6PD related to dehydroepiandrosterone (DHEA) Williams and Boehm [47] synthesised an allenic sulfone derivate, which was found to bind covalently to the allosteric site of G6PD. Interestingly, we performed the docking of this compound in the same way as done for KPF–CoA, and found the same optimal site for these two structurally closed compounds. Moreover we are thus able to explain the mechanism proposed in [47]: K475 would be ''the basic amino acid residue'' supposed responsible for the ''tautomerisation of the propargylic moiety of the inhibitor, which would be rapidly trapped by a nucleophilic residue'', this later being precisely T333 (or S331), as appearing from the molecular docking (data not shown).

In the present study, we have shown that carboxylic NSAIDs, e.g. KPF, do not inhibit G6PD directly, but *via* its CoA metabolite. Human and Yeast G6PD were inhibited, and we used the yeast enzyme to gain further information on the interaction. We demonstrate that this binding was irreversible, and that the binding site is in the environment of C316 in Yeast G6PD. The human enzyme does not bear cysteine at this position, but a hydrophobic cavity exists in the same domain, and other nucleophilic residues might play the same role (Ser, Thr).

Side-effects of KPF-racemate were attributed alternatively to the *S*-enantiomer as an inhibitor of COX, or to the *R*-enantiomer as an inhibitor of beta-oxidation. The present study gives new insights into the side effects of NSAIDs by revealing a new target for the metabolite KPF–CoA, namely G6PD, an enzyme essential in the regulation of the redox potential in cells. The original property of these metabolites we describe here for the first time, should explain the lowered levels of NADPH and GSH, associated to the production of ROS described above, which leads to the apoptosis of gastro-intestinal cells observed both in cancer regression and in ulcer formation after administration of these drugs. Further studies will be needed to assess the role of G6PD as a key enzyme for

regulation of oxidative stress *in vivo*. Nevertheless these results will open a novel approach to the treatment of NSAID-induced gastrointestinal side-effects by administration of antioxidant drugs.

Acknowledgments

The authors would thank Etienne Benoît (Ecole Vétérinaire de Lyon) and Eric Battaglia (Université de Metz) for helpful discussions. This work was supported by the Association de Recherche sur la Polyarthrite Rhumatoïde (ARP), Paris, the Centre Hospitalier Régional Universitaire de Nancy (CPRC grant), the Centre National de la Recherche Scientifique (CNRS) and the Ministère de l'Education Nationale, de la Recherche et de la Technologie (thesis grant of CA).

REFERENCES

[1] Smith CJ, Zhang Y, Koboldt CM, Muhammad J, Zweifel BS, Shaffer A, et al. Pharmacological analysis of cyclooxygenase-1 in inflammation. Proc Natl Acad Sci USA 1998;95:13313–8.
[2] Newberry RD, Stenson WF, Lorenz RG. Cyclooxygenase-2-dependent arachidonic acid metabolites are essential modulators of the intestinal immune response to dietary antigen. Nat Med 1999;5:900–6.
[3] Carabaza A, Suesa N, Tost D, Pascual J, Gomez M, Gutierrez M, et al. Stereoselective metabolic pathways of ketoprofen in the rat: incorporation into triacylglycerols and enantiomeric inversion. Chirality 1996;8:163–72.
[4] Jamali F, Brocks DR. Clinical pharmacokinetics of ketoprofen and its enantiomers. Clin Pharmacokinet 1990;19:197–217.
[5] Carabaza A, Cabre F, Rotllan E, Gomez M, Gutierrez M, Garcia ML, et al. Stereoselective inhibition of inducible cyclooxygenase by chiral nonsteroidal anti-inflammatory drugs. J Clin Pharm 1996;36:505–12.
[6] Cooper SA, Reynolds DC, Reynolds B, Hersh EV. Analgesic efficacy and safety of (R)-ketoprofen in postoperative dental pain. J Clin Pharm 1998;38:11S–8S.
[7] Nieto AI, Cabre F, Moreno FJ, Alarcon de la Lastra C. Mechanisms involved in the attenuation of intestinal toxicity induced by (S)-(+)-ketoprofen in re-fed rats. Dig Dis Sci 2002;47:905–13.
[8] Kusuhara H, Komatsu H, Sumichika H, Sugahara K. Reactive oxygen species are involved in the apoptosis induced by nonsteroidal anti-inflammatory drugs in cultured gastric cells. Eur J Pharm 1999;383:331–7.
[9] Thun MJ. Aspirin and gastrointestinal cancer. Adv Exp Med Biol 1997;400:395–402.
[10] Levoin N, Blondeau C, Guillaume C, Grandcolas L, Chrétien F, Jouzeau J-Y, et al. Elucidation of the mechanism of inhibition of cyclooxygenases by acyl-coenzyme A and acylglucuronic conjugates of ketoprofen. Biochem Pharm 2004;68:1957–69.
[11] Kawaguchi A, Bloch K. Inhibition of glucose 6-phosphate dehydrogenase by palmitoyl coenzyme A. J Biol Chem 1974;249:5793–800.
[12] Levoin N, Chrétien F, Lapicque F, Chapleur Y. Synthesis and biological testing of Acyl-CoA-ketoprofen conjugates as selective irreversible inhibitors of COX-2. Bioorg Med Chem 2002;10:753–7.
[13] Maire-Gauthier R, Buronfosse T, Magdalou J, Herber R, Besse S, Delatour P, et al. Species-dependent enantioselective glucuronidation of carprofen. Xenobiotica 1998;28:595–604.
[14] Noltmann EA, Gubler CJ, Kuby SA. Glucose 6-phosphate dehydrogenase (Zwischenferment). I. Isolation of the crystalline enzyme from yeast. J Biol Chem 1961;236:1225–30.
[15] Özer N, Aksoy Y, Ogus IH. Kinetic properties of human placental glucose-6-phosphate dehydrogenase. Int J Biochem Cell Biol 2001;33:221–6.
[16] Heurtaux T, Benani A, Bianchi A, Moindrot A, Gradinaru D, Magdalou J, et al. Redox state alteration modulates astrocyte glucuronidation. Free Rad Biol Med 2004;37:1051–63.
[17] Stanton RC, Seifter JL, Boxer DC, Zimmerman E, Cantley LC. Rapid release of bound glucose-6-phosphate dehydrogenase by growth factors. Correlation with increased enzymatic activity. J Biol Chem 1991;266:12442–8.
[18] Au SW, Gover S, Lam VM, Adams MJ. Human glucose-6-phosphate dehydrogenase: the crystal structure reveals a structural NADP(+) molecule and provides insights into enzyme deficiency. Structure Fold Des 2000;8:293–303.
[19] Kotaka M, Gover S, Vandeputte-Rutten L, Au SW, Lam VM, Adams MJ. Structural studies of glucose-6-phosphate and $NADP^+$ binding to human glucose-6-phosphate dehydrogenase. Acta Crystallogr D Biol Crystallogr 2005;61:495–504.
[20] Rowland P, Basak AK, Gover S, Levy HR, Adams MJ. The three-dimensional structure of glucose 6-phosphate dehydrogenase from *Leuconostoc mesenteroides* refined at 2.0 A resolution. Structure 1994;2:1073–87.
[21] Cosgrove MS, Gover S, Naylor CE, Vandeputte-Rutten L, Adams MJ, Levy HR. An examination of the role of Asp-177 in the His-Asp catalytic dyad of *Leuconostoc mesenteroides* glucose 6-phosphate dehydrogenase: X-ray structure and pH dependence of kinetic parameters of the D177N mutant enzyme. Biochemistry 2000;39:15002–11.
[22] Taketa K, Pogell BM. The effect of palmityl coenzyme A on glucose 6-phosphate dehydrogenase and other enzymes. J Biol Chem 1966;241:720–6.
[23] Levy HR, Vought VE, Yin X, Adams MJ. Identification of an arginine residue in the dual coenzyme-specific glucose-6-phosphate dehydrogenase from *Leuconostoc mesenteroides* that plays a key role in binding $NADP^+$ but not NAD^+. Arch Biochem Biophys 1996;326:145–51.
[24] Levoin N. Métabolites réactifs des anti-inflammatoires non-stéroïdiens: bases structurales de leurs interactions avec les cibles protéiques impliquées dans les processus inflammatoires. PhD Thesis 2002. Université Henri Poincaré Nancy 1, Nancy.
[25] Scopes RK. Allosteric control of *Zymomonas mobilis* glucose-6-phosphate dehydrogenase by phosphoenolpyruvate. Biochem J 1997;326:731–5.
[26] Vought V, Ciccone T, Davino MH, Fairbairn L, Lin Y, Cosgrove MS, et al. Delineation of the roles of amino acids involved in the catalytic functions of *Leuconostoc mesenteroides* glucose 6-phosphate dehydrogenase. Biochemistry 2000;39:15012–21.
[27] Anderson BM, Wise DJ, Anderson CD. *Azotobacter vinelandii* glucose 6-phosphate dehydrogenase properties of NAD- and NADP-linked reactions. Biochim Biophys Acta 1997;1340:268–76.
[28] Kirkman HN, Gaetani GF. Regulation of glucose-6-phosphate dehydrogenase in human erythrocytes. J Biol Chem 1986;261:4033–8.
[29] Riganti C, Gazzano E, Polimeni M, Costamagna C, Bosia A, Ghigo D. Diphenyleneiodonium inhibits the cell redox

metabolism and induces oxidative stress. J Biol Chem 2004;279:47726–31.
[30] Jain M, Brenner DA, Cui L, Lim CC, Wang B, Pimentel DR, et al. Glucose-6-phosphate dehydrogenase modulates cytosolic redox status and contractile phenotype in adult cardiomyocytes. Circ Res 2003;93:e9–16.
[31] Kawamori T, Rao CV, Siebert K, Reddy BS. Chemopreventive activity of celecoxib, a specific cyclooxygenase-2 inhibitor, against colon carcinogenesis. Cancer Res 1998;58:409–12.
[32] Wechter WJ, Kantoci D, Murray ED, Quiggle DD, Leipold DD, Gibson KM, et al. R-flurbiprofen chemoprevention and treatment of intestinal adenomas in the APC(Min)/+mouse model: implications for prophylaxis and treatment of colon cancer. Cancer Res 1997;57:4316–24.
[33] Piazza GA, Alberts DS, Hixson LJ, Paranka NS, Li H, Finn T, et al. Sulindac sulfone inhibits azoxymethane-induced colon carcinogenesis in rats without reducing prostaglandin levels. Cancer Res 1997;57:2909–15.
[34] Tatebe S, Sinicrope FA, Kuo MT. Induction of multidrug resistance proteins MRP1 and MRP3 and gamma-glutamylcysteine synthetase gene expression by nonsteroidal anti-inflammatory drugs in human colon cancer cells. Biochem Biophys Res Commun 2002;290:1427–33.
[35] Mahmud T, Rafi SS, Scott DL, Wrigglesworth JM, Bjarnason I. Nonsteroidal antiinflammatory drugs and uncoupling of mitochondrial oxidative phosphorylation. Arthritis Rheum 1996;39:1998–2003.
[36] Browne GS, Nelson C, Nguyen T, Ellis BA, Day RO, Williams KM. Stereoselective and substrate-dependent inhibition of hepatic mitochondria beta-oxidation and oxidative phosphorylation by the non-steroidal anti-inflammatory drugs ibuprofen, flurbiprofen, and ketorolac. Biochem Pharm 1999;57:837–44.
[37] Kemal C, Casida JE. Coenzyme A esters of 2-aryloxyphenoxypropionate herbicides and 2-arylpropionate antiinflammatory drugs are potent and stereoselective inhibitors of rat liver acetyl-CoA carboxylase. Life Sci 1992;50:533–40.
[38] Knights KM, Drew R. The effects of ibuprofen enantiomers on hepatocyte intermediary metabolism and mitochondrial respiration. Biochem Pharm 1992;44:1291–6.
[39] Uyemura SA, Santos AC, Mingatto FE, Jordani MC, Curti C. Diclofenac sodium and mefenamic acid: potent inducers of the membrane permeability transition in renal cortex mitochondria. Arch Biochem Biophys 1997;342:231–5.
[40] Tian WN, Braunstein LD, Pang J, Stuhlmeier KM, Xi QC, Tian X, et al. Importance of glucose-6-phosphate dehydrogenase activity for cell growth. J Biol Chem 1998;273:10609–17.
[41] Ayene IS, Stamato TD, Mauldin SK, Biaglow JE, Tuttle SW, Jenkins SF, et al. Mutation in the glucose-6-phosphate dehydrogenase gene leads to inactivation of Ku DNA end binding during oxidative stress. J Biol Chem 2002;277:9929–35.
[42] Szweda LI, Uchida K, Tsai L, Stadtman ER. Inactivation of glucose-6-phosphate dehydrogenase by 4-hydroxy-2-nonenal. Selective modification of an active-site lysine. J Biol Chem 1993;268:3342–7.
[43] Ciftci M, Buyukokuroglu ME, Kufrevioglu OI. Effect of cefaperazone/sulbactam and ampicillin/sulbactam on the in vitro activity of human erythrocyte glucose-6-phosphate dehydrogenase. J Basic Clin Physiol Pharm 2001;12:305–13.
[44] Ciftci M, Ozmen I, Buyukokuroglu ME, Pence S, Kufrevioglu OI. Effects of metamizol and magnesium sulfate on enzyme activity of glucose 6-phosphate dehydrogenase from human erythrocyte in vitro and rat erythrocyte in vivo. Clin Biochem 2001;34:297–302.
[45] Jeffery J, Hobbs L, Jornvall H. Glucose-6-phosphate dehydrogenase from *Saccharomyces cerevisiae*: characterization of a reactive lysine residue labeled with acetylsalicylic acid. Biochemistry 1985;24:666–71.
[46] Marks PA, Banks J. Inhibition of mammalian glucose-6-phosphate dehydrogenase by steroids. Proc Natl Acad Sci USA 1960;46:447–52.
[47] Williams JR, Boehm JC. The synthesis and reactivity of β,γ-acetylenic and allenic sulfoxides and sulfones of dehydroepiandrosterone and their reactions with 1-butanethiol and glucose-6-phosphate dehydrogenase. Bioorg Med Chem Lett 1992;2:933–6.